Journal of Colloid and Interface Science 649 (2023) 559–570

Contents lists available at ScienceDirect

Journal of Colloid And Interface Science

journal homepage: www.elsevier.com/locate/jcis

Theory of adsorption of ethoxylates at the water | oil and water | air interfaces. 1. Monolayers of single-component and Poisson distributed alkylphenol ethoxylates

Radomir I. Slavchov

Queen Mary University of London, School of Engineering and Materials Science, Mile End Road, London E1 4NS, United Kingdom

GRAPHICAL ABSTRACT

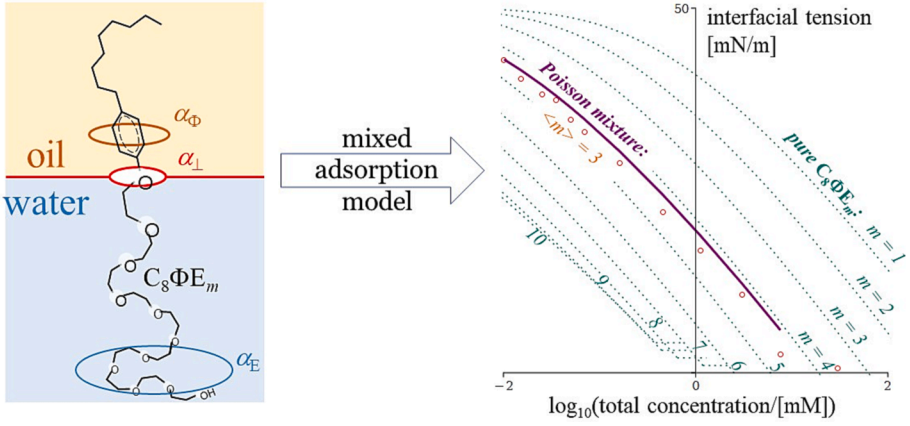

ARTICLE INFO

Keywords:
Adsorption
Liquid interfaces
Nonionic surfactants
Ethoxylated surfactants
Surface phase transition
Lateral attraction parameter
Surfactant mixtures
Poisson distributed surfactants

ABSTRACT

Currently, the bulk thermodynamic properties of an arbitrary liquid mixture of oligomers are accessible with reasonable accuracy through popular 3D statistical models (SAFT, Flory-Huggins) under a wide range of conditions. These models are implemented in widely available software suites used for process design. The hypothesis investigated here is that the same is, in principle, achievable with monolayers of mixed surfactants on liquid surfaces. A molecular thermodynamic theory of the adsorption of alkylphenoxypolyethoxyethanols, $C_nH_{2n+1}C_6H_4(OC_2H_4)_mOH$, on fluid interfaces is presented. It covers homologues of $m = 0$–10; water|alkane and water|gas interfaces; single surfactants and surfactant mixtures. The adsorption behaviour has been predicted as a function of the structure of the ethoxylated surfactants and the model has been validated against tensiometric data for forty systems. All values of the adsorption parameters have been either predicted, independently determined, or at least compared to a theoretical estimate. The single surfactant parameters have been used to predict the properties of 'normal' Poisson distributed mixtures of ethoxylates, in good agreement with literature

E-mail address: r.slavchov@qmul.ac.uk.

https://doi.org/10.1016/j.jcis.2023.06.068
Received 19 April 2023; Received in revised form 5 June 2023; Accepted 11 June 2023
Available online 19 June 2023

data. Partitioning between water and oil, micellization, solubility and surface phase transitions are also discussed.

Nomenclature

C	surfactant concentration, [m^{-3}] or [mM]
K_a	equilibrium adsorption constant (from the aqueous phase), [m]
K_{a0}	K_a at $m = 0$ according to Eqs. (23)–(24), [m]
K_p	equilibrium partition coefficient, K_p = concentration(oil)/concentration(water)
k	Boltzmann constant, [J/K]
L_{CH2}	London constant for lateral interaction between two methylene groups, [m^6J]
l_{CH2}	length of a $–CH_2–$ group along the hydrophobic chain, [m]
l_E	length of a $–OC_2H_4–$ segment, [m]
l_Φ	length of a phenylene segment, [m]
m	number of $–C_2H_4O–$ units in the ethoxy chain of C_nE_m and $C_n\Phi E_m$
m_0	transition unit number (at $m > m_0$, $\alpha = \alpha_E$; otherwise, $\alpha = \alpha_\Phi$)
n	number of $–CH_2–$ units in the alkyl chain in C_nE_m and $C_n\Phi E_m$
n_{CH2}	equivalent number of methylene groups in the hydrophobic chain in C_nE_m and $C_n\Phi E_m$
R_β	attraction radical of the sticky disc model, eq. (3)
r	disc area ratio ($r = \alpha_{10}/\alpha_4$ for a mixture of $C_8\Phi E_4$ and $C_8\Phi E_{10}$)
T	temperature, [K]
$x_\perp$	empirical increment $d\alpha_\perp/da_m m$
$\propto$	disc area of the surfactant molecule ($\approx\alpha_{collapse}/1.10$), [$m^2$]
$\alpha_{collapse}$	collapse area for a spread monolayer, [m^2]
α_E	cross-sectional area of the E_m segment, [m^2]
$\alpha_{Langmuir}$	site area of Langmuir's model, [m^2]
α_m	increment of the disc area of the E_m segment with m, $d\alpha_E/dm = 2.985$ Å^2
α_{OH}	cross-sectional area of alkanols, 16.5 Å^2
α_Φ	cross-sectional area of the $–C_2H_4–C_6H_4–O–C_2H_4–$ segment, [m^2]
$\alpha_\perp$	area of neat interface lost upon adsorption of a molecule, Eq. (22), [m^2]
β	lateral attraction parameter
β_{osm}	effective contribution of the solvent osmotic effect to β
β_{vdW}	contribution of the London dispersion interaction to β
Γ	adsorption of the surfactant, [m^{-2}] or [mol/m^2]
γ^S	surface activity coefficient of the surfactant
$\Delta\mu_{CH2}$	hydrophobic free energy of transfer of $–CH_2–$ form oil or gas phase to water, [J]
$\Delta\mu_E$	free energy of transfer of $–C_2H_4O–$ form water to oil or gas phase, [J]
$\Delta\mu_\Phi$	hydrophobic free energy of transfer of $–C_6H_4–$ form oil or gas phase to water, [J]
δ_a	adsorption length, Eq. (21), [m]
π^S	surface/interfacial pressure of the monolayer, $\pi^S \equiv \sigma_0 - \sigma$, [J/$m^2$]
σ	surface/interfacial tension of the monolayer, [J/m^2]
σ_0	surface/interfacial tension of the neat surface (at $\psi = 0$), [J/m^2]
ψ	$\equiv \alpha\Gamma$ is the surface fraction covered by surfactant
2D	two-dimensional
CMC	critical micelle concentration, [mM]
C_nE_m	alkanol polyethoxylate, $C_nH_{2n+1}(OC_2H_4)_mOH$
$C_n\Phi E_m$	alkylphenol polyethoxylate, $C_nH_{2n+1}C_6H_4(OC_2H_4)_mOH$
$C_n\Phi E_{<m>}$	a mixture of $C_n\Phi E_m$ of average head size $<m>$
EoS	equation of state
HFL	the model of 1-component hard-disc fluid of Helfand, Frisch and Lebowitz
LHP	the model of multicomponent hard-disc fluid of Lebowitz, Helfand and Praestgaard
MTD	molecular thermodynamic
NPB	the model of multicomponent hard-disc fluid with attraction of Nikas, Puvvada and Blankschtein
SD	sticky disc adsorption model
W|G	water|gas surface
W|O	water|oil interface

1. Introduction

Many common nonionic surfactants are made of an alkyl tail bound in a certain way to a polyethoxy chain, e.g., alkanol polyethoxylates ($C_nH_{2n+1}(OC_2H_4)_mOH$ or C_nE_m for short), alkylphenol polyethoxylates ($C_nH_{2n+1}C_6H_4(OC_2H_4)_mOH$ or $C_n\Phi E_m$ for short), polysorbates, poloxamers etc., which all have the -$(OC_2H_4)_mOH$ segment (or -E_m) acting as the polar head group. The modification of the length m of the polyethylene glycol chain allows the formulation specialists to optimize the physico-chemical properties of a surfactant for a specific application: one has options to increase or decrease the surface activity, the partition coefficient K_p, the critical micelle concentration (*CMC*) or the solubility, to alter the shape of the micelles, the steric repulsion in thin films etc.

The experimental data suggest that ethoxylation makes surfactants more water-soluble – K_p changes by a factor of 2.9 per -OC_2H_4- unit [1]. The dependence of *CMC* or solubility on m is also known [2,3]. However, the available tensiometric data show that the extent of ethoxylation has a complex effect on the surface activity at both water|gas (W|G) and water|oil (W|O) interfaces: at low surface coverage, surfactants of larger m adsorb more (suggesting adsorption constant K_a increasing with m), but at high coverages, the opposite trend is observed (due to the increased lateral repulsion in the monolayer between bulker -E_m). This leads to a characteristic intersection of the isotherms of homologues of different m and the same alkyl chain length n [2,4]. These findings are empirical – to our knowledge, no in-depth molecular thermodynamic (MTD) model exists to rationalize them and to establish rules to predict the effect of m on the adsorption parameters.

The behaviour of some C_nE_m homologues at W|G has been reported to be captured well by a two-dimensional (2D) fluid model for hard discs with short-range attraction [5,6], in the sense that all adsorption parameters matched their theoretically expected values. Importantly, this includes mixtures of C_nE_m homologues [5]. However, neither the dependence of the adsorption parameters on m has been investigated systematically, nor the adsorption at W|O has been studied from the same modellistic point of view. The knowledge about the related phenomenon of 2D phase behaviour of these surfactants' monolayers is completely empirical [7,8], compared to the well-understood 2D gas–liquid phase transitions of simple nonionic surfactants at W|G [9] and 2D liquid–solid transitions of fluorinated alcohols at W|O [10]. Moreover, 2D fluid theories of adsorption are actually not popular – researchers in the field still prefer the Langmuir-Szyszkowski model and

its derivatives [11–13], despite the fact that localized theories like Langmuir's have essential disadvantages compared to nonlocalized one, especially for W|O [9,6]. Furthermore, the lateral dispersion attraction between the adsorbed surfactants at W|G is often ignored [11,12,14], which is reasonable for high homologues but not for $m < 6$ [5,6].

Broadly speaking, a set of MTD models for micellization, partition and adsorption of mixtures of surfactants has the potential to become a common instrument for process simulation of disperse systems containing surfactants. This situation can be compared to what thermodynamic models of liquid mixtures did for chemical process engineering in general: modern process design is difficult to imagine without tools like Aspen, based on liquid mixture models to predict properties, phase behaviour, partitioning etc. Until surface thermodynamic models for surfactant mixtures are developed, the chemical industry will continue to rely on empirical rules such as HLB to navigate the design of surfactant formulations. Towards the aim of demonstrating the potential of the MTD approach, in a series of three papers, we will show that a family of hard-disc fluid models describes well the available adsorption data for ethoxylated nonionic surfactants, and all adsorption parameters can be predicted with reasonable accuracy for both W|G and W|O interfaces. In the current work (part 1 of the series), we demonstrate this on the example of $C_nΦE_m$ homologues (limiting ourselves to $m \leq 10$). This builds up on previous work on fatty alcohols and acids, phosphineoxides, betaines, and fluorinated alcohols [6,9,10]. It also extends existing work on $C_nΦE_m$ mixtures at silica|water [15,16] to liquid interfaces. In the second paper of the series, we will investigate the adsorption of C_nE_m and will discuss the behaviour of longer homologues. In part 3, we will show that these thermodynamic models allow the type and the stability of a water–oil emulsions to be predicted via theoretical stability maps (type of stability vs concentration and oil fraction at varying m and n), in agreement with the results from dedicated experiments – i.e. surface thermodynamic modelling can indeed be used for process simulation involving dispersions.

For more than five decades, $C_nΦE_m$ surfactants such as *n*-octylphenol and n-nonylphenol polyethoxylates, and the branched octylphenol polyethoxylates of the Triton X class, have been used at an industrial scale for applications varying from household detergents to crude oil production [17]. Lately, their use declines due to environmental concerns: $C_nΦE_m$ tend to degrade via partial hydrolysis of the -E_m segment, producing short homologues ($C_nΦE_{0–2}$) that are toxic [18]. As a result, the current interest towards $C_nΦE_m$ is directed to wastewater treatment problems and fate in the body of the short homologues at low concentration. The understanding of $C_nΦE_m$ adsorption on W|G is important for the design of wastewater treatment processes involving gas bubbles (foam fractionation, bubble columns and possibly ozonation). The adsorption on W|O, on the other hand, is a surrogate for understanding the interaction of $C_nΦE_{0–2}$ with biomembranes and hydrophobic particles.

$C_nΦE_m$ will probably remain in industrial use for specialist applications (e.g., [19–22]) due to their low price and unique properties – in particular, they have high affinity to 'difficult' interfaces such as silica|water [23,16]. Our interest towards $C_nΦE_m$ is, however, most of all academic: this is a well-studied class of ethoxylated surfactants. High-quality tensiometric data exist for the purified homologues in well-characterized W|G and W|O systems – in particular, the extensive work by Crook et al. [1,2]. We could not find C_nE_m data of the same range and quality for W|O. The comparison between W|O and W|G is an important test for the thermodynamic models and makes their parametrization easier [9], because a hard disc model ideally has transferable parameters, i.e. the molecular area for W|O and W|G, at least for simple surfactants, are the same, and a simple relationship exists between the adsorption constants at W|G and W|O [9]. Importantly, the latter allows to predict the solvent effect of the oil phase on the adsorption, which mainly affects the adsorption constant [24,9].

We start with a summary of the 2D hard-disc fluid theory of liquid monolayers, with minor generalizations to accommodate the three-block structure of $C_nΦE_m$ into the MTD models of the adsorption parameters (predicting the adsorption constant K_a, the hard disc area of the adsorbed molecule α, and the lateral attraction parameter β as functions of m). In *sec.* 3, we compare the theory with the data for $C_8ΦE_m$ by Crook et al. [1,2], including W|G, W|O, mixtures of two surfactants, and technical mixtures $C_8ΦE_{<m>}$ with a Poisson distribution of m.

2. Theory

2.1. Equation of state

Single surfactant at W|O: the model of Helfand, Frisch, and Lebowitz (HFL). On W|O, nonionic surfactants of large cross-sectional area behave as a 2D hard-disc fluid [6], because no significant dispersion interaction exists between the surfactant hydrocarbon chains when immersed in a hydrocarbon medium [25]. An accurate surface equation of state (EoS) for a single-component fluid monolayer made of hard discs has been derived by Helfand, Frisch and Lebowitz using the apparatus of the scaled particle theory [26]:

$$\alpha\pi^S/kT = \psi/(1-\psi)^2. \tag{1}$$

Here, $\pi^S \equiv \sigma_0 - \sigma$ is the interfacial pressure of the monolayer, σ is interfacial tension in the presence of surfactant; σ_0 is tension of the neat interface (at $\psi = 0$); $\psi = \alpha\Gamma$ is surface coverage; Γ is adsorption; α is the hard disc area of the surfactant molecule. The surface activity coefficient γ^S corresponding to eq. (1) follows from the Gibbs isotherm $\mathrm{d}(\alpha\pi^S/kT) = \psi\mathrm{d}\ln(\gamma^S\psi)$:

$$\ln\gamma^S = -\ln(1-\psi) + \psi(3-2\psi)/(1-\psi)^2. \tag{2}$$

The HFL model (1)-(2) is suitable to monolayers of nonionic [9] and (in combination with Gouy's equation) ionic surfactants [24] at W|O.

Single surfactant at W|G: the sticky disc (SD) model. At W|G, the $C_nΦE_m$ monolayers become cohesive due to the lateral attraction between the hydrocarbon tails in the air. A reliable delocalized EoS for 2D fluid made of attracting molecules is the sticky disc model of Ivanov et al. [9,27,28]:

$$\frac{\alpha\pi^S}{kT} = \frac{R_\beta - 1}{2\beta(1-\psi)}, \qquad R_\beta \equiv \sqrt{1 + 4\beta\frac{\psi}{1-\psi}}. \tag{3}$$

The respective surface activity coefficient γ^S that follows from the Gibbs isotherm is [9]:

$$\ln\gamma^S = -\ln(1-\psi) + \left(2 + \frac{1}{\beta}\right)\ln\frac{2}{1+R_\beta} + \frac{\psi(4-3\psi)}{(1-\psi)^2}\frac{2}{1+R_\beta}. \tag{4}$$

Eqs. (3)–(4) simplify to the HFL model when $\beta = 0$. A similar extension of the HFL model to take into account the attraction has been proposed by Parsons [29], via an empirical correction $-\beta\psi^2$ in the HFL EoS (1) (see S8 in the supplementary information).

The surface activity coefficients (2) or (4) determine the adsorption isotherms (Γ vs C) of the HFL and SD models:

$$K_a C = \gamma^S\Gamma, \tag{5}$$

where K_a [m] is the adsorption constant of the surfactant. Eq. (5) assumes that the aqueous solution is dilute enough to behave as ideal; this assumption often fails nearby the *CMC*, due to the appearance of surfactant dimers and trimers (leading to a characteristic inflection in the σ vs ln C dependence right below *CMC*).

A mixture of surfactants at W|O: the model of Lebowitz, Helfand, and Praestgaard (LHP). Crook et al. reported tensiometric data for well-defined binary mixtures of $C_8ΦE_4$ and $C_8ΦE_{10}$ [2]. A mixed adsorbed layer at W|O can be treated as a hard-disc mixture. The EoS for a mixture of discs of different areas has been derived by Lebowitz, Helfand and Praestgaard (LHP) [30]; for the two-component case, their *eq. 6.7* can be written as

$$\frac{\alpha_{10}\pi^S}{kT} = \frac{\psi_{10} + r\psi_4 - (\sqrt{r}-1)^2\psi_4\psi_{10}}{(1-\psi_4-\psi_{10})^2}. \tag{6}$$

Here, $\psi_m \equiv \alpha_m\Gamma_m$ is the surface fraction covered by each surfactant; $r \equiv \alpha_{10}/\alpha_4$ is the disc area ratio for $C_8\Phi E_{10}$ and $C_8\Phi E_4$. The Gibbs isotherm relates this EoS to the surface activity coefficients γ_m^S of the two components:

$$\mathrm{d}\frac{\pi^S}{kT} = \Gamma_4 \mathrm{dln}\left(\gamma_4^S\psi_4\right) + \Gamma_{10}\mathrm{dln}\left(\gamma_{10}^S\psi_{10}\right). \tag{7}$$

For a binary mixture, both γ_4^S and γ_{10}^S can be derived from Eq. (7) as:

$$\ln\gamma_4^S = -\ln(1-\psi_4-\psi_{10}) + \frac{\psi_4(3-2\psi_4) + \psi_{10}\left[\frac{2}{\sqrt{r}}(1-\psi_{10}) + \frac{1-\psi_4}{r} - 3\psi_4\right]}{(1-\psi_4-\psi_{10})^2};$$

$$\ln\gamma_{10}^S = -\ln(1-\psi_4-\psi_{10}) + \frac{\psi_{10}(3-2\psi_{10}) + \psi_4[2\sqrt{r}(1-\psi_4) + r(1-\psi_{10}) - 3\psi_{10}]}{(1-\psi_4-\psi_{10})^2}. \tag{8}$$

This specifies the two adsorption isotherms for this binary mixture:

$$\alpha_4 K_{a4} C_4 = \frac{\psi_4}{1-\psi_4-\psi_{10}} \mathrm{e}^{\frac{\psi_4(3-2\psi_4)+\psi_{10}\left[\frac{2}{\sqrt{r}}(1-\psi_{10})+\frac{1-\psi_4}{r}-3\psi_4\right]}{(1-\psi_4-\psi_{10})^2}};$$

$$\alpha_{10} K_{a10} C_{10} = \frac{\psi_{10}}{1-\psi_4-\psi_{10}} \mathrm{e}^{\frac{\psi_{10}(3-2\psi_{10})+\psi_4[2\sqrt{r}(1-\psi_4)+r(1-\psi_{10})-3\psi_{10}]}{(1-\psi_4-\psi_{10})^2}}. \tag{9}$$

The LHP theory (modified to accommodate lateral attraction) has been used by Nikas et al. [5] to model the mixed adsorption layer of two C_nE_m surfactants at W|G; by Fraser et al. [31] to analyse the case of a surfactant that assumes two configurations of different disc areas at the surface; and by our group to model the osmotic effect from the solvent molecules penetrating into the surfactant monolayer [6]. To our knowledge, it has not been compared to data for mixed surfactant monolayers at W|O, although LHP is an obvious choice for such systems.

Crook et al. also studied experimentally numerous cases of mixtures of $C_n\Phi E_m$ of wide distribution of m [2]. For a general mixture of M components, the LHP EoS reads [30]:

$$\frac{\pi^S}{kT} = \frac{\sum\Gamma_m}{1-\sum\psi_m} + \frac{\pi(\sum R_m\Gamma_m)^2}{(1-\sum\psi_m)^2}. \tag{10}$$

Here, the sums are over $m = 1\ldots M$ and R_m is the hard disc radius of the m-th homologue ($\alpha_m = \pi R_m{}^2$). The respective activity coefficients have been derived from the Gibbs isotherm by Nikas et al. [5]:

$$\ln\gamma_m^S = -\ln\left(1-\sum\psi_i\right) + \frac{\alpha_m\sum\Gamma_i + 2\pi R_m\sum R_i\Gamma_i}{1-\sum\psi_i} + \frac{\pi\alpha_m(\sum R_i\Gamma_i)^2}{(1-\sum\psi_i)^2}. \tag{11}$$

They specify M adsorption isotherms for M surfactants: $K_{a,m}C_m = \gamma_m{}^S\Gamma_m$, $m = 1\ldots M$. We will use eq. (10)-(11) to simulate the behaviour of $C_n\Phi E_m$ mixtures having a Poisson distribution of m.

A mixture of surfactants at W|G: the model of Nikas, Puvvada, and Blankschtein (NPB). Unfortunately, the SD model (3) has not been generalized to mixtures yet. On the other hand, the Parsons EoS has been extended to mixtures by Nikas et al. [5] – their model is presented in S8. For surfactants of small lateral attraction parameter, the Parsons model is nearly equivalent to SD [6,9], and therefore, the NPB model should be sufficiently accurate for ethoxylate mixtures.

2.2. Adsorption parameters

The EoS from *sec*. 2.1 approximate the shape of the lateral interaction potential between the adsorbed molecules to a solid particle repulsion (Heaviside function) and short-range uniform sticky attraction (Dirac function). All adsorption parameters of eq. (1)-(5) – K_a, α, β – have a clear physical meaning and can be determined independently or calculated with reasonable accuracy from relatively simple MTD models or from independent experimental data, as discussed below. The geometry of the octylphenol polyethoxylates is complicated compared to the surfactants we studied previously [9,6,10] so the homologous $C_n\Phi E_m$ series offers an important test of this set of models.

The **hard disc area** α is a measure of the lateral repulsive interaction between the adsorbed molecules: this includes direct steric, chain overlap, and (when water binds strongly to the polar group) short-range hydration repulsion. For hard-disc fluid models, it has been shown previously that the value of α agrees with empirical crystallographic data and collapse data for insoluble monolayers [9,6,10]. It can also be accurately calculated from rotational isomeric state simulation [5], or even – at least for simple surfactants – straight from the geometry of the molecule [10,32]. Moreover, the value of α has been shown to be transferable, i.e. it is the same for W|G and W|O [6,9]. In contrast, the popular adsorption models of Langmuir and Volmer and their derivatives [9] use an area parameter which should be treated as empirical when applied to liquid surfaces: $\alpha_{Langmuir}$ and α_{Volmer} are larger than the crystallographic areas, and are nontransferable – the fitted values for W|G data do not work for W|O [9].

For $C_8\Phi E_m$ of m larger than, e.g., 5–6, the repulsion is controlled by the maximum cross-sectional area α_E of the oligomeric E_m chain, see Fig. 1. To find α_E, we determined the collapse areas from the Langmuir trough data for C_nE_m at W|G by Islam and Kato [33] and Lange and Jeschke [7] (the collapse was assumed to occur at the highest reported

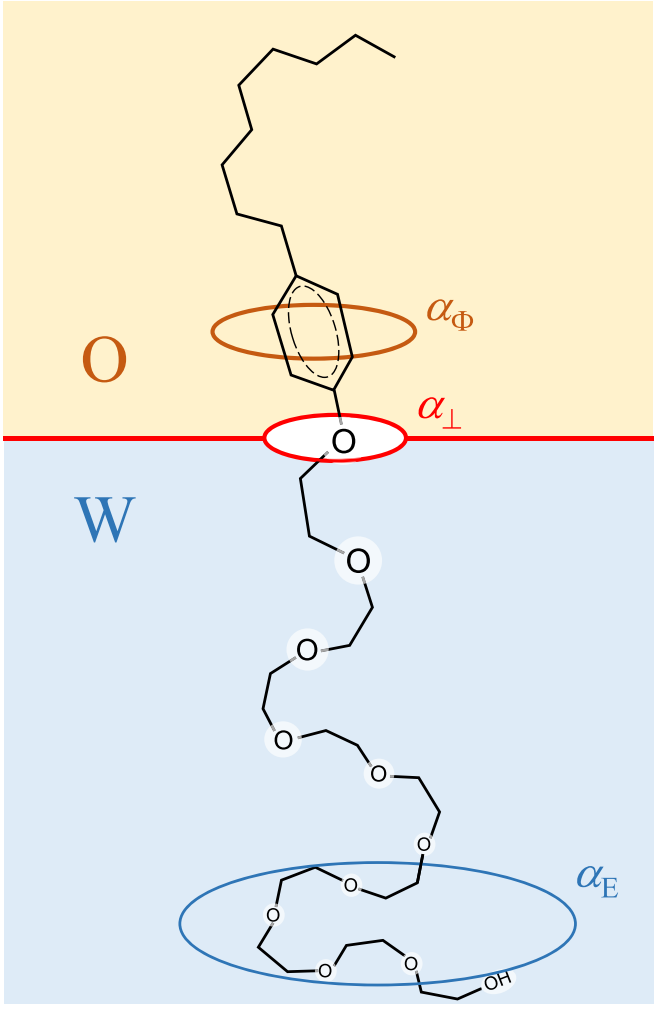

Fig. 1. A schematic of the assumed geometry of an adsorbed $C_8\Phi E_m$ molecule.

surface pressure). The collapse area of C_nE_m follows a linear dependence on m; the corresponding disc area can be expressed as

$$\alpha_E = \alpha_{OH} + \alpha_m m, \tag{12}$$

where $\alpha_{OH} = 16.5$ Å^2 and $\alpha_m = 2.99 \pm 0.12$ Å^2 (see details in S1). The result (12) has been previously shown to work well for C_nE_6 [6]. This dependence encompasses empirically all repulsive interactions (steric direct, steric via chain overlap, hydration); it disagrees with the theoretical power laws $\alpha_E = const \times m^{1/2}$ of Van Voorst Vader [34] or $\alpha_E = const \times m^{6/11}$ of Sedev [35]. Eq. (12) is a linear regression over data for homologues of m = 1–10, and perhaps these power laws will be approached at larger m, where the chain overlap is expected to be the leading effect. Indeed, extrapolation of eq. (12) to $m > 10$ leads to overestimated α_E (see S1).

In contrast, for short polyethoxylate chains, the disc area of adsorbed $C_n\Phi E_m$ molecules is controlled by the benzene ring and its substituents – this is the area α_Φ in Fig. 1, standing for the projection of the segment –C_2H_4–C_6H_4–O–C_2H_4–. Unlike α_E, the area α_Φ is independent of m. The disc area α of any $C_8\Phi E_m$ can be assumed to be the larger of the two molecular projected segment areas α_Φ and α_E, i.e.

$$\alpha = \max(\alpha_\Phi, \alpha_E) \tag{13}$$

We considered also other hypotheses; one alternative, $\alpha = \max(\alpha_\Phi, \alpha_E)^{1/2}\alpha_E^{1/2}$ (corresponding to an elliptic projection), was found to be quite reasonable and it compares well to the experiment, but eq. (13) works better (see S1). The dependence (13) of α on m is discontinuous. To smoothen it, we used the nearly equivalent function

$$\alpha = \alpha_{OH} + \frac{1}{2}\alpha_m\left\{m + m_0 + \frac{1}{2}\ln[2\cosh(2m - 2m_0)]\right\} \tag{14}$$

where

$$m_0 = (\alpha_\Phi - \alpha_{OH})/\alpha_m \tag{15}$$

is the transition unit number: for $m < m_0$, α_Φ dominates the repulsion; otherwise, α_E does. The smoothening has little effect on the predicted areas α or on the optimal dispersion of the adsorption model from the experimental data; however, it removes the stepwise change of the dispersion value with the variation of the optimization parameters, which simplifies the optimization procedure. Moreover, a smooth transition is likely to be closer to reality.

We will treat α_Φ as a free parameter because we were unable to find data for collapse of insoluble monolayers of $C_n\Phi E_{1\ldots3}$ – but we can still put some limits on it. Adam [36] reported data for monolayers of insoluble alkylphenols, $C_n\Phi OH$, that collapse at 23 Å^2, corresponding to $\alpha = 21$ Å^2 (with the geometrical correction factor 1.10 for the difference between the disc area and the hexagonal cell in a packed structure). This agrees with the geometry of alkylphenol, with benzene ring of axis 6.4 Å (distance between beta carbon atoms plus a Van der Waals diameter of a CH segment) and a mean Van der Waals diameter of 4.6 Å for the alkyl – if the expected tilt of the benzene ring is ignored, this corresponds approximately to an ellipse of area $\pi \times 6.4 \times 4.6/4 = 23$ Å^2. This is a lower bound for the area of $C_n\Phi E_{1\ldots3}$. Adding to it the contributions from the projection of the -O-C_2H_4- segment, allowing for rotation of the benzene ring and adding a tilt can increase α_Φ to ~ 30–35 Å^2.

Lateral attraction parameter β at W|G. An important feature of the SD EoS (3) is that it agrees with the theoretically expected virial expansion [9]:

$\pi^S/kT = \Gamma + B_2\Gamma^2$, with surface second virial coefficient

$$B_2 = 2\alpha - \alpha\beta, \tag{16}$$

a formula rigorously valid for attracting hard discs (which can be viewed as a definition of β). The 2α term in eq. (16) is the repulsive hard-disc part of the virial coefficient, and $\alpha\beta$ is the attractive part. The attraction is assumed to be controlled mainly by two contributions [6]: the dispersion attraction between the hydrocarbon chains of the surfactant through air (producing β_{vdW}) and the relatively small osmotic contribution from the solvent present in the monolayer (β_{osm}):

$$\beta = \beta_{vdW} + \beta_{osm}. \tag{17}$$

The lateral attraction parameter β is expected to be small for monolayers at W|O, based on data for other surfactants at W|O [6]. Even at W|G, β of $C_n\Phi E_m$ is not very large for the higher homologues, since both β_{vdW} and β_{osm} decrease steeply with the increase of the disc area α. However, at W|G, the first few homologues ($C_n\Phi E_{0\text{-}5}$, which are the most interesting ones from the viewpoint of wastewater treatment) exhibit a significant lateral attraction.

For β_{vdW} at W|G, one can use the following formula derived for two interacting upstanding hydrocarbon chains [6,9]:

$$\beta_{vdW} = \frac{\pi}{\tilde{\alpha}\int_{2\sqrt{\tilde{\alpha}/\pi}}^{\infty}\left[\exp\left(\frac{3\arctan\frac{1}{\tilde{r}+\frac{\tilde{r}}{2}}}{4\tilde{T}\tilde{r}^5}\right) - 1\right]\tilde{r}d\tilde{r}}, \quad \text{where}$$

$$\tilde{T} = n_{CH_2}^4 l_{CH_2}^6 kT \Big/ L_{CH_2}, \quad \tilde{\alpha} = \alpha \Big/ n_{CH_2}^2 l_{CH_2}^2. \tag{18}$$

Here, $L_{CH2} = 4.24 \times 10^{-78}$ m^{6}J is the London constant for the interaction between two methylene groups, and $l_{CH2} = 1.26$ Å is the length of a –CH_2– group along the hydrophobic chain [25]; n_{CH2} is the equivalent number of methylene groups in the hydrophobic chain. The phenylene group -C_6H_4- will be treated as approximately six methylene groups, i.e. we will assume that $n_{CH2} = 14$ for $C_8\Phi E_m$. For reference, the derivation of eq. (18) is presented in S2.

For the dependence on α of the second term in Eq. (17) – the osmotic contribution β_{osm} – we will use the following regression formula:

$$\beta_{osm} = \alpha_\beta/\alpha, \tag{19}$$

where the value $\alpha_\beta = 16.15$ Å^2 produces β_{osm} that agrees well with the available experimental data from ref. [6], see Table 1.

The sticky disc model (3)-(4) with β computed from Eq. (17) has been found before to agree very well with surface tension data for many simple surfactants at W|G [6], including C_nE_6; therefore, we will attempt to treat it as an established dependence to calculate (rather than fit) β. We will show below that that this works well for higher $C_n\Phi E_m$ homologues, but when close contact between the phenylene groups is possible (for $m < 5$), deviations occur corresponding to additional attraction. The source of this may be a phenylene-phenylene quadrupole Keesom interaction, as discussed in S2.

For the **equilibrium constant K_a of adsorption** from the aqueous solution to W|O or W|G, we will use Ivanov's MTD model, the main features of which were developed in ref. [37,24], and which, after a straightforward generalization, was extended to three-block structures [10]. The latter generalization can be applied to $C_n\Phi E_m$, and gives for the adsorption constant the formula:

$$K_a = \delta_a \exp\left(\frac{n\Delta\mu_{CH_2}}{kT} + \frac{\Delta\mu_\Phi}{kT} + \frac{\alpha_\perp\sigma_0}{kT}\right). \tag{20}$$

Here, the hydrophobic contribution to the adsorption free energy comes from **(i)** $\Delta\mu_{CH2}$, the hydrophobic free energy to transfer a methylene group form the nonaqueous phase to water ($\Delta\mu_{CH2} = 1.39kT$ for oil and $1.04kT$ for air [9]), and **(ii)** the respective $\Delta\mu_\Phi$ for phenylene. The

Table 1
Comparison between the regression formula (19) with $\alpha_\beta = 16.15$ Å^2 and experimental values of β_{osm} from ref. [6].

	α[Å^2]	β_{osm} from ref. [6]	β_{osm} from Eq. (19)
alkanols	16.5	0.98	0.98
alkanoic acids at low pH	18	0.84	0.90
C_nE_6	34.3	0.5	0.47

contribution from the hydrophobic energy of the terminal methyl group is approximately $\Delta\mu_{CH3} \approx 2\Delta\mu_{CH2}$ [9], but, at least for alkyl tails [6,9,10], the extra $1 \times \Delta\mu_{CH2}$ is cancelled by the polarization effect of the polar head group on the alpha carbon atom from the hydrophobic tail – hence the factor in front of $\Delta\mu_{CH2}$ remains n in Eq. (20).

The preexponential factor δ_a in Eq. (20) is the so-called adsorption length and stands for the translational and rotational degrees of freedom lost upon adsorption. For a hydrophilic-lyophilic centre located between the phenylene and -E_m segments, it is given by

$$\delta_a = \frac{kT}{2}\left(\frac{l_\Phi}{\Delta\mu_\Phi} + \frac{l_E}{\Delta\mu_E}\right) \tag{21}$$

Here, l_Φ is the length in direction normal to the surface of the phenylene segment (≈ 4.2 Å, from bond geometry); l_E is the length of a –OC_2H_4– segment (≈ 3.5 Å, from bond geometry); $\Delta\mu_E > 0$ is the energy of transfer of –OC_2H_4– from water to air or oil.

Finally, the area $\alpha_\perp$ in eq. (20) stands for the surfactant-free W|G or W|O interface that disappears upon adsorption of a $C_n\Phi E_m$ molecule, see Fig. 1. If the –E_m segment were rigid and remained completely immersed in water, the area $\alpha_\perp$ would be approximately equal to that of the first –OC_2H_4– segment, which is similar to $\alpha_\perp$ of an alcohol. Therefore, $\alpha_{\perp,\min} = 1.10 \times \alpha_{OH}$, where α_{OH} is the hard disc area of an alcohol (the same that appears in Eq. (12) for α_E). However, –OC_2H_4– is hydrophobic enough to cover some of the surface; were the shape of the E_m block a perfect cylinder, this situation would correspond to $\alpha_{\perp,\max} = 1.10 \times \alpha_E = 1.10 \times \alpha_{OH} + 1.10 \times \alpha_m m$ (with α_E from Eq. (12)). For the assumed conical trapezoid geometry of E_m in Fig. 1, we expect behaviour in between the two limits ($1.10 \times \alpha_{OH}$ and $1.10 \times \alpha_{OH} + 1.10 \times \alpha_m m$), where $\alpha_\perp$ still increases with m but the increment is smaller than $1.10 \times \alpha_m$, i.e.

$$\alpha_\perp = 1.1 \times a_{OH} + x_\perp a_m m \tag{22}$$

where the empirical increment $x_\perp$ must be between 0 and 1.10.

Eqs. (20)–(22) lead to an explicit formula for the dependence of K_a on m:

$$\ln K_a = \ln K_{a0} + x_\perp \frac{a_m \sigma_0}{kT} m, \text{ with intercept (23)}$$

$$\ln K_{a0} = \ln\left(\frac{l_\Phi}{2}\frac{kT}{\Delta\mu_\Phi} + \frac{l_E}{2}\frac{kT}{\Delta\mu_E}\right) + \frac{n\Delta\mu_{CH_2}}{kT} + \frac{\Delta\mu_\Phi}{kT} + 1.10\frac{a_{OH}\sigma_0}{kT}. \tag{24}$$

According to this formula, **(i)** $K_a(m)$ is exponential; **(ii)** both the slope and the intercept depend explicitly on the nature of the interface – first because of σ_0 (σ_0 = 72.0 mJ/m^2 for W|G and 50.1 mJ/m^2 for water|isooctane), and second, because the transfer energies $\Delta\mu_i$ in Eq. (24) are different for gas and oil. The formula (24) for the intercept involves significant approximations, while the interfacial tensions predicted by our adsorption models are sensitive to the parameter K_{a0}; therefore, when dealing with data, we will treat K_{a0} as a fitting parameter, using Eq. (24) as a reference point to discuss how reasonable the experimental K_{a0} values are.

In emulsions, $C_n\Phi E_m$ homologues of large n and small m will partition completely to the oil phase. In this case, the adsorption constant K_a^O for a surfactant from the oil phase to W|O is more relevant than the out-of-water constant K_a. The two are related through the partition coefficient,

$$K_p \equiv C^O/C = K_a/K_a^O, \tag{25}$$

where C^O is the concentration of surfactant in the oil in equilibrium with the aqueous solution of concentration C. Eq. (25) ignores surfactant association in the two bulk phases.

The **partition coefficients K_p** of $C_8\Phi E_m$ between water and isooctane were determined by Crook et al. [1]. According to their data, all homologues but $C_8\Phi E_9$ and $C_8\Phi E_{10}$ partition preferentially to the oil phase ($K_{p1\text{-}8} > 1$). We used the experimental values of K_p for all following calculations. However, we also analysed the dependence $\ln K_p$ vs m in order to estimate the transfer free energies $\Delta\mu_i$ appearing in eq. (24). The experimental dependence of $\ln K_p$ on m for octylphenol polyethoxylates from ref. [1] is linear (see S3):

$$(C_8\Phi E_m \text{ at W|isooctane}) \quad \ln K_p = 9.27 - 1.077m. \tag{26}$$

We compare the experimental dependence to the following MTD model of K_p (which follows from the same assumptions of Ivanov et al. [10] that produce the formulae for the adsorption constants above):

$$(C_n\Phi E_m \text{ at W|O}) \quad \ln K_p \equiv \ln\frac{K_a}{K_a^O} = \frac{(n+1)\Delta\mu_{CH_2}}{kT} + \frac{\Delta\mu_\Phi}{kT} - \frac{m\Delta\mu_E}{kT} - \frac{\Delta\mu_{OH}}{kT}; \tag{27}$$

$$(C_nE_m \text{ at W|O}) \quad \ln K_p \equiv \ln\frac{K_a}{K_a^O} = \frac{(n+1)\Delta\mu_{CH_2}}{kT} - \frac{m\Delta\mu_E}{kT} - \frac{\Delta\mu_{OH}}{kT}. \tag{28}$$

(i) Comparison of eq. (26) and (27) shows that $\Delta\mu_E/kT = 1.077$ for transfer from isooctane to water.

(ii) Eq. (26) predicts for octylphenol ($m = 0$) the value $\ln K_p\{C_8\Phi OH\} = 9.27$. This value can be compared with the one for octanol between octane and water, $\ln K_p\{C_8OH\} = 3.58$ (see *eq. 46* in the SI of ref. [9]). Comparison of the values of $\ln K_p\{C_8\Phi OH\}$ and $\ln K_p\{C_8OH\}$ with the difference between Eq. (27) and (28) gives $\Delta\mu_\Phi/kT = 9.27\text{–}3.58 = 5.69$.

This specifies all parameters in eq. (24) for K_a at W|O. It is more difficult to find the energies $\Delta\mu_E/kT$ and $\Delta\mu_\Phi/kT$ for transfer between water and gas, as values of the respective Henry's constants are not readily available. We will limit ourselves to an estimate: since we know that for methylene $\Delta\mu_{CH2}(W|G) = 0.75 \times \Delta\mu_{CH2}(W|O)$ [9], we will assume that the same ratio holds for $\Delta\mu_E$ and $\Delta\mu_\Phi$, i.e. for air $\Delta\mu_E(W|G)/kT = 0.75 \times 1.077 = 0.81$ and $\Delta\mu_\Phi(W|G)/kT = 0.75 \times 5.69 = 4.27$. Substituting these values in Eq. (24), we predict $\ln(K_{a0}/[m]) = -3.3$ for W|O and $\ln(K_{a0}/[m]) = -6.3$ for W|G.

3. Results and discussion

A single $C_8\Phi E_m$ homologue at W|O. Crook et al. [2] reported interfacial tension of water|isooctane vs the initial concentration C_0 in the aqueous phase (before partitioning) of pure octylphenol polyoxyethylates (m = 1–10) at 25 °C. They used equal volumes of water and oil, therefore, the surfactant concentration C in the aqueous phase after partition equilibrium has been reached is given by

$$C = C_0/(1 + K_p). \tag{29}$$

We used the experimental values of K_p [1] to convert C_0 to C, and the interfacial tension of the neat water|isooctane, σ_0 = 50.1 mJ/m^2, to convert the interfacial tensions σ to interfacial pressures $\pi^S = \sigma_0 - \sigma$.

The data for $\pi^S(C; m)$ was compared to the HFL model (1)-(2) for $\pi^S(C;K_a,\alpha)$ combined with the MTD models (23) for $K_a(m)$ and (14) for $\alpha(m)$. There are three parameters left free to fit: the intercept $\ln K_{a0}$, the empirical $x_\perp$, and the disc area α_Φ of the -C_2H_4-C_6H_4-O-C_2H_4- segment (or equivalently, the transition unit number m_0, see Eq. (15)). The merit function we used for the regression has the form:

$$dev^2(K_{a0}, x_\perp, m_0) = \frac{\sum_{m,i}\left[\pi^S_{m,i} - \pi^S_{th}(C_i, m; K_{a0}, x_\perp, m_0)\right]^2}{N - 3}, \tag{30}$$

where $\pi^S_{m,i}$ is the i^{th} experimental value for the homologue $C_8\Phi E_m$; π^S_{th} is the theoretical value following from the HFL model (1)-(2) at the i^{th} experimental surfactant concentration C_i, with K_a given by Eq. (23) and α given by Eq. (14). The sum is over all ten homologues and datapoints, a total of N = 108 points $\{C_i,m,\pi^S_{m,i}\}$ (only those below the *CMC*/solubility limit are used).

There are several issues with the data that need to be considered when the results are discussed. The first one is that the more oil-soluble homologues, and $C_8\Phi E_1$ and $C_8\Phi E_2$ in particular, are of concentration in the aqueous phase that is so low that the experimental K_p is of high uncertainty (which we estimated at ±40%). The second problem is that the short homologues (up to $C_8\Phi E_5$ – see the discussion for W|G below) may have a non-negligible lateral attraction parameter β (osmotic and quadrupolar, see S2). However, it is quite difficult to distinguish between the effects from the inaccurate K_p and from the neglected β, and our attempts to take them into account did not lead to convincing results. A third problem with the short ethoxylates is that Crook et al. reported that some of their stock solutions were in the form of a dispersion, which may result in very slow equilibration. The final issue is that the data for $C_8\Phi E_8$ at W|O appears to be an artifact as it does not follow the trends of all other homologues.

The optimized parameter values are reported in Table 2. The results are reasonable: the fitted $\ln(K_{a0}/[\mathrm{m}]) = -3.11$ is close to the theoretical −3.3 from eq. (24), and both $x_\perp$ and α_Φ are of values in the expected range. The tensiometric data are compared to the model in Fig. 2 for some of the homologues, in coordinates π^S vs C and π^S vs lg C, and for all ten homologues in S5. The adsorption model correctly captures the main features of the adsorption data:

(i) small change in the overall shape of the surface tension isotherms as m increases from 2 to 5, but with an increase in the adsorption constant (the initial slope);
(ii) significant change in the shape of the isotherms at $m > 5$ (where α_E becomes larger than α_Φ) indicative of altered lateral repulsion, with a further increase in the adsorption constant.

This simultaneous increase in α and K_a causes the isotherms of the low homologues to cross those of the high ones: the larger K_a of, e.g., $C_8\Phi E_{10}$ produces stronger adsorption than $C_8\Phi E_2$ in the dilute concentration region. However, due to the repulsion between the bulky E_{10} groups, $C_8\Phi E_2$ adsorbs more at high concentration (Fig. 2-right).

Comparison with other adsorption models at W|O. We previously [9] did an extensive comparison of the delocalized (i.e. fluid-based) hard disc models of HFL and SD with the more popular models of Langmuir-Szyszkowski (which is localized, i.e. a site model), Volmer (a model of delocalized 1D hard-rod fluid), Frumkin (Langmuir with empirical attraction), Van der Waals (Volmer with empirical attraction), and Parsons (HFL with empirical attraction). For C_nE_6, we also [6] compared SD with the two-state model of Fainerman and Miller [13] (also localized – cf. the liquid version in ref. [31]). In most cases, as regression models, these were found to be indiscernible – if the same number of fitting parameters is used, the produced dispersions are nearly the same. However, the area parameter matches the crystallographic and collapse values only for 2D delocalized models, and the attraction parameter β matches the theoretical value (17)–(19) only in the case of the SD model. The 2D liquid description was found to be particularly convincing in the case of W|O systems because there β is small and the real system indeed approaches a perfect 2D hard-disc fluid [9,6].

To reiterate the points made in ref. [9,6], here we compare the HFL model at W|O with the most popular adsorption model without lateral attraction: the one of Langmuir-Szyszkowski. It has the same two parameters as HFL: adsorption constant K_a and area $\alpha_{Langmuir}$ (although this is a site or cell area rather than hard disc area). To make the two regressions as similar as possible, we use a similar merit function to Eq. (30) for the three dimensional data set $\{m,C_i,\pi^S_{m,i}\}$ by Crook et al. However, in this case the area must be treated as an empirical value – it cannot be expected that $\alpha_{Langmuir}$ is equal to the one from Eq. (12) corresponding to monolayer collapse. For the site area parameter α_{OH} of alcohols on various water|oil interfaces, the value 39 Å^2 has been found [9] and can be used. The increment α_m in Eq. (12), however, has to be treated as a free parameter, i.e. the merit function is

$$dev^2(K_{a0}, x_\perp, \alpha_m, m_0) = \frac{\sum_{m,i}\left[\pi^S_{m,i} - \pi^S_{th}(C_i, m; K_{a0}, x_\perp, \alpha_m, m_0)\right]^2}{N-4}. \quad (31)$$

This time, π^S_{th} is set by Szyszkowski's formula, $kT/\alpha_{Langmuir} \times \ln(1 + \alpha_{Langmuir}K_aC)$. As usual, the result from the regression is decent – Langmuir-Szyszkowski has the right shape to pass through the data, and Henry's region is model-independent [9]. Nevertheless, despite the additional fourth fitting parameter in eq. (31), the goodness of the fit is worse than that of HFL (dev = 1.75 vs 1.65 mJ/m^2). What is more important is that the values of the parameters make less sense. The best fit value of $\ln(K_{a0}/[\mathrm{m}])$ is −3.75 ± 0.4 (vs −3.11 ± 0.4 for HFL and −3.3 from theory). The empirical area ratio $x_\perp = 0.18$ is similar to that of HFL. The areas α_m and α_Φ, however, are very large (4.7 and 64 Å^2, respectively) and difficult to compare to the actual molecular geometry in the dense monolayer close to the collapse. Of course, one can use the theoretical result that, for liquid monolayers, Langmuir's site area should be twice the geometrical [9], but then, one may also consider the theoretical expectation that a liquid monolayer is better described by a 2D liquid model like HFL than a site model like Langmuir's.

Mixture of two homologues at W|O. Crook et al. [2] reported adsorption data for mixtures of $C_8\Phi E_4$ and $C_8\Phi E_{10}$. Based on the single surfactant adsorption isotherms, these homologues have adsorption constants $K_{a4} = 0.07112$ m and $K_{a10} = 0.1426$ m, and areas $\alpha_4 = 32.67$ Å^2 and $\alpha_{10} = 46.35$ Å^2, from the parameters in Table 2 and Eqs. (14) and (23). Using these parameters in the LHP model, Eqs. (6) and (9), allows us to predict the surface tension at any composition of the aqueous solution, i.e. any two concentrations C_4 of $C_8\Phi E_4$ and C_8 of $C_8\Phi E_{10}$.

Crook et al. [2] used as a variable the initial total concentration in the aqueous phase, $C_0 = C_{0,4} + C_{0,10}$, before partitioning, at different values of the fraction $x_{10} = C_{0,10}/C_0$. To compare their data and the theory in the original coordinates, we used that

$$C_4 = C_{0,4}/(1 + K_{p4}) = (1 - x_{10})C_0/(1 + K_{p4});$$

$$C_{10} = C_{0,10}/(1 + K_{p10}) = x_{10}C_0/(1 + K_{p10}). \quad (32)$$

Substituting these into Eq. (9), together with Eq. (6), we end up with three equations for three unknowns – ψ_4, ψ_{10}, and π^S – as functions of C_0 at a fixed x_{10}. These are solved numerically. The results are shown in Fig. 3.

The predicted curves agree reasonably well with the experiment. The comparison can be improved greatly by using the isotherms fitted to each homologue rather than those obtained from the total fit (30) over the whole homologous series (which has an averaging effect). However, such 'improvement' may obscure the actual reason for the slight discrepancy – possibly the ignored β_4, or admixtures of a higher homologue in $C_8\Phi E_4$ (which is suggested by the change in curvature of the π^S vs C_0 dependence at low C_0, see Fig. 3), or even a small error in K_{p10}. Actually, the experiment is not very well designed as under the studied conditions most of $C_8\Phi E_4$ is extracted by the isooctane and all mixed monolayers are dominated by $C_8\Phi E_{10}$ – see Fig. 3-right; as a result, a small error in the value of K_{p10} has a larger effect than a big error in any of the adsorption parameters.

Technical $C_n\Phi E_{<m>}$ at W|O: multiple components with Poisson distribution of m. The usual synthetic routes for ethoxylates produce mixtures of wide distribution of the head group size m [38]. Very often,

Table 2
Adsorption parameters for octylphenyl polyoxyethylene ethers.

	water|isooctane (m = 1–10)	water|gas (m = 6–10)
$\ln(K_{a0}/[\mathrm{m}])$	−3.11 ± 0.4 (vs −3.3 from Eq. (24))	−6.66 ± 0.05 (vs −6.3 from Eq. (24))
$x_\perp$	0.32 ± 0.12	
α_Φ (and m_0)	32.7 ± 2 Å^2 (and m_0 = 5.42 ± 0.7, from Eq. (15))	
dev	1.65 mJ/m^2	0.36 mJ/m^2

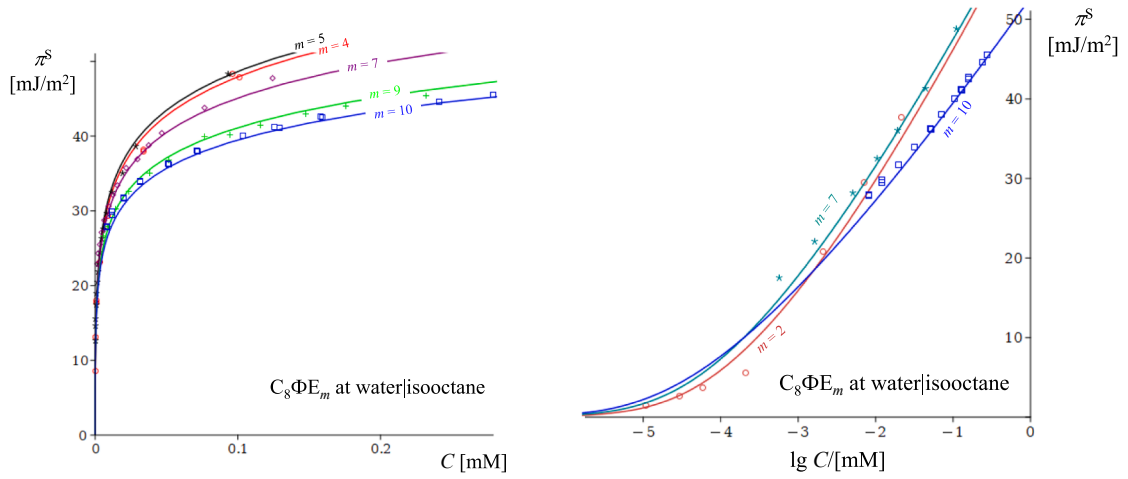

Fig. 2. Comparison of the HFL model (1)-(2) with tensiometric data for adsorption $C_8\Phi E_m$ on water|isooctane by Crook et al. [2].

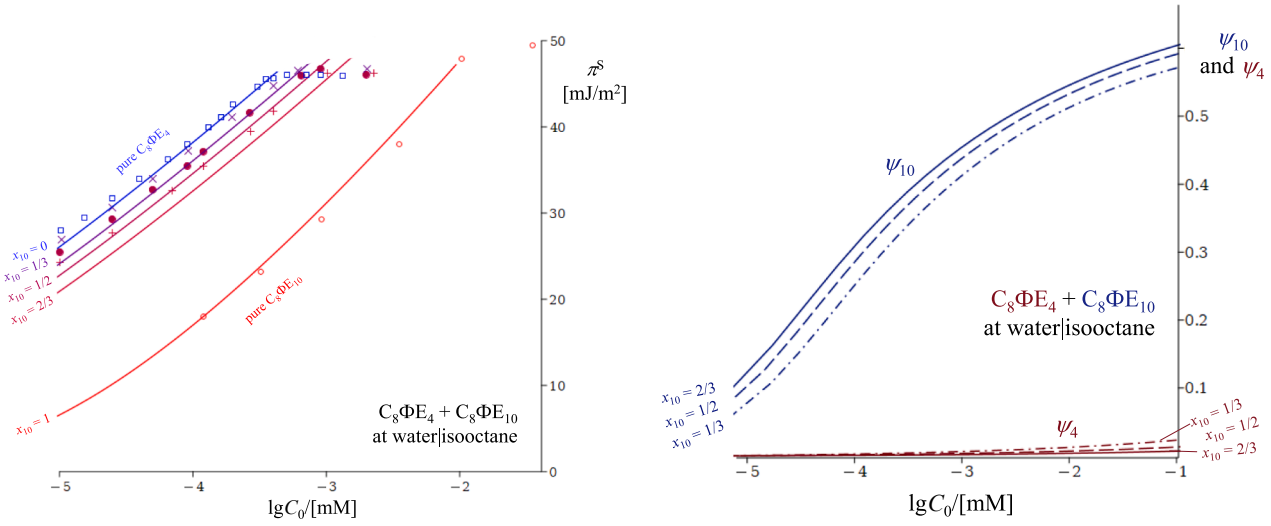

Fig. 3. Left: comparison of the LHP mixed hard-disc fluid model to the tensiometric data (interfacial pressure π^S vs initial total surfactant concentration in water C_0) of Crook et al. [2] for adsorption of $C_8\Phi E_4 + C_8\Phi E_{10}$ at water|isooctane (at several fractions x_{10} of $C_8\Phi E_{10}$ in the total system). **Right:** respective composition of the mixed adsorbed layer, in terms of coverages $\psi_m = \alpha_m \Gamma_m$. The monolayers are dominated by $C_8\Phi E_{10}$.

the probability distribution of m follows to a good approximation the theory of Flory [39], i.e. the Poisson distribution holds,

$$x_m = e^{1-<m>} \frac{(<m>-1)^{m-1}}{(m-1)!}. \tag{33}$$

Crook et al. [2] reported data for mixtures $C_8\Phi E_{<m>}$ with Poisson distributed m (they referred to them as 'normal distribution $C_8\Phi E_{<m>}$' but did not mean Gaussian x_m [2,38]). Thus, concentration C_0 of $C_8\Phi E_{<m>}$ correspond to the following homologue concentrations before and after partitioning:

$$C_{0,m} = x_m C_0;$$

$$C_m = C_{0,m}/(1+K_{p,m}) = x_m C_0/(1+K_{p,m}), \qquad m = 1\ldots\infty, \tag{34}$$

with x_m from eq. (33). Since the adsorption and partition parameters of the homologues of $m > 10$ are undetermined, we lump the high-end of the distribution into a single virtual component of $m = 10$, that is, we assume that components of $m = 10\ldots\infty$ behave as $C_8\Phi E_{10}$. The concentrations (34) define completely the surface composition $\psi_{1\text{-}10}$ through the respective adsorption isotherms, eq. (11), and the

Table 3
Adsorption parameters of $C_8\Phi E_m$.

m	K_a [m], Eq. (23)		α [Å^2], Eq. (14)	β, Eqs. (17)-(19)
	W|G	W|O	W|G & W|O	W|G
1	[a] 2D solid?	0.05023	32.67	[a] 2D solid?
2	[a] 2D solid?	0.0564	32.67	[a] 2D solid?
3	0.002114	0.06334	32.67	[b] 4.39 ([c] 2.20)
4	0.002496	0.07112	32.67	[b] 3.67 ([c] 2.13)
5	0.00295	0.07986	32.8	[b] 2.57 ([c] 2.06)
6	0.003486	0.08968	34.48	[c] 1.78
7	0.004115	0.1007	37.4	[c] 1.45
8	0.004863	0.1131	40.38	[c] 1.21
9	0.005742	0.127	43.37	[c] 1.03
10	0.006785	0.1426	46.35	[c] 0.89

[a] On W|G, the first two homologues behave differently from the rest, likely due to a phase transition to 2D solid. [b] Lateral attraction parameter obtained from a single-parametric fit of the data for the respective surfactant and fixed values of K_a and α. [c] Lateral attraction parameter calculated from Eqs. (17)–(19).

adsorption parameters $K_{a,m}$ and α_m of the single homologues in Table 3. The substitution of the so-obtained $\psi_{1\text{-}10}$ into the EoS (10) of the LHP model gives us the interfacial tension value σ. A sample procedure for this computation is given in S9 as a ready-to-use Maple code.

The results for the nine Poisson distributed $C_8\Phi E_{<m>}$ of Crook et al. are shown in Fig. 4. The agreement is more than adequate, especially in view of the approximations made. Significant deviations appear only for $<m> = 2$–3 close to the break, which is due to the neglected lateral attraction parameter $\beta_{1\text{-}3}$; some $C_8\Phi OH$ may also be present in the mixture [2]. Deviations are observed also for $<m> = 4$–7 at the lowest studied concentration, where it appears that the technical $C_8\Phi E_{<m>}$ again adsorbs more than the model predicts (2–3 mJ/m^2 difference). However, we are not convinced that the experimental data in this region can be trusted – similar deviations are observed with some, but not all, of the pure surfactants reported by Crook (e.g., $m = 7$ in S5), and may be due to dioctylphenol adducts present [1,2,38]. Altering slightly the distribution away from Poisson's (33) can easily make the comparison perfect.

The results for $C_8\Phi E_{<2>}$ and $C_8FE_{<3>}$ are compared to the HFL model for the pure $C_8\Phi E_2$ and $C_8\Phi E_3$ (dashed lines in Fig. 4), to demonstrate the effect of polydispersity. For these two homologues, the effect is significant. Its cause is mostly the difference in the partition coefficient – the lower homologues ($C_8\Phi E_{1\text{-}2}$) present in the two mixtures $C_8\Phi E_{\langle 2\text{-}3\rangle}$ tend to get extracted by the isooctane phase, which reduces the actual concentration of octylphenol ethoxylates in the aqueous phase compared to C_0. The distribution of the mixture of surfactants between water, oil and interface is discussed further in S7; the code in S9 allows it to be calculated.

A single $C_8\Phi E_m$ homologue at W|G. Crook et al. [2] reported the surface tension σ of aqueous solutions of the same ten pure octylphenyl polyoxyethylene ethers, $C_8\Phi E_{1\text{-}10}$. We used the surface tension of neat W|G, $\sigma_0 = 72.0$ mJ/m^2, to calculate the respective surface pressures π^S. The experimental data for $\pi^S(C; m)$ were compared to the SD model (3)–(5) for $\pi^S(C;K_a,\alpha,\beta)$ (allowing for cohesion), combined with the MTD models (23) for $K_a(m)$, (14) for $\alpha(m)$, and (17)–(19) for the lateral attraction parameter $\beta(m)$. We assume that the area is unchanged compared to W|O, so $\alpha(m)$ is known (see values in Table 3). In addition, Eq. (17)–(19) for $\beta(m)$ are explicit so it is also known. Finally, we assume that the empirical geometrical parameter $x_\perp = 0.32$ that appears in Eq. (23) (the presumably constant ratio between the penetrated surface area $\alpha_\perp$ and the area α_E of the –E$_m$ segment in Fig. 1) is also unchanged compared to W|isooctane – note, however, that the slope of lnK_a vs m increases due to the larger value of σ_0 in eq. (23), 72 instead of 50 mJ/m^2. A single parameter is left unknown for the whole series: the intercept lnK_{a0}. Thus, the merit function we used for the regression over the W|G data has the form:

$$dev^2(K_{a0}) = \frac{\sum_{m,i}\left[\pi^S_{m,i} - \pi^S_{th}(C_i, m; K_{a0})\right]^2}{N-1}, \tag{35}$$

where π^S_{th} is the theoretical value following from the SD model (3)–(5) at the i^{th} experimental surfactant concentration C_i, with K_a given by Eq. (23), α from (14) and β from (17)–(19).

The initial analysis demonstrated two important features displayed by the W|G data of Crook et al. that do not allow eq. (35) to be applied to homologues of small m. The first one is that the short homologues that approach the area $\alpha = \alpha_\Phi$ appear to have lateral interaction much stronger than the one predicted by eq. (17)-(19) – i.e. for $m \le 5$, there is a missing interaction in our model (17)–(19) for β. A likely candidate for it is the short-range quadrupole–quadrupole attraction between the benzene rings, see S2. Indeed, Eq. (18) with $n_{CH2} = 14$ treats the benzene-benzene attraction as a London interaction decaying as $\propto 1/r^6$, while the quadrupole–quadrupole interaction decays as $\propto 1/r^5$ (see S2 and *table I* in ref. [40]). The second issue – possibly due to the same interaction – is that the first two homologues behave very differently from the rest of the series. We believe that the reason is a phase transition from 2D liquid state of the monolayer to a 2D crystalline one. Similar phase transition has been observed in fluorinated alkanols at water|hexane [21], and with dodecanol, $C_{14}E_1$, $C_{16}E_2$ and $C_{18}E_3$ at W|G [7,8,22,41]. In S4, we present additional evidence for the validity of this hypothesis from the analysis of the data of *CMC*/solubility vs m.

To deal with these two issues, we first fitted only the data of Crook et al. for $m > 5$, which are apparently unaffected by the quadrupole–quadrupole interaction ($N = 62$ points). The agreement is excellent – within the experimental error. The parameter value obtained by minimization of eq. (35) where the sum is over the data for $C_8\Phi E_{6\text{-}10}$ is $\ln(K_{a0}/[m]) = -6.66 \pm 0.05$. The obtained $\ln(K_{a0}/[m])$ agrees reasonably well with the theoretical estimate −6.3 from Eq. (24).

Next, to quantify the missing lateral (possibly quadrupole) attraction, we compared the SD model to the data for $C_8\Phi E_3$, $C_8\Phi E_4$, $C_8\Phi E_5$ separately. For these three homologues, we used the value of K_a predicted by Eq. (23) with $K_{a0} = \exp(-6.66)$ as obtained for $m > 5$, and the area from eq. (14). This leaves an unknown β for each of $C_8\Phi E_3$, $C_8\Phi E_4$, and $C_8\Phi E_5$. The optimization leads to $\beta_3 = 4.39$, $\beta_4 = 3.63$, and $\beta_5 = 2.57$ (compared to 2.20, 2.13, and 2.06 following from Eq. (17)–(19) – see also the comparison in S6).

All adsorption parameter values are reported in Table 2 and Table 3. The surface tension data are compared to the SD model in Fig. 5 for all homologues but the first two ($C_8\Phi E_1$ and $C_8\Phi E_2$ are assumed to form 2D solid monolayer and require a different EoS, see ref. [10]).

We also considered data for $C_n\Phi E_m$ at W|G by other authors [4,42]. Unfortunately, the results from different groups disagree with each other. For example, Schick et al. and Sahoo et al. report results for $C_9\Phi E_{15}$ that disagree by a factor of 5 in the concentration, and for $C_9\Phi E_{10}$ the disagreement is by a factor of 10. The data of Schick et al. for $C_9\Phi E_{10}$ and $C_9\Phi E_{16}$ agree reasonably well with those of Crook et al. for $C_8\Phi E_{10}$ and $C_8\Phi E_{16}$, when scaled for the difference of one methylene group (see ref. [9]); they also agree well with the adsorption model presented above. Among the three sets [2,4,42], only the work of Crook et al. covers homologues of $m < 10$, and we anyway intend to investigate higher homologues in a following work (data for C_nE_m of large m are more abundant) as their areas deviate from eq. (22) (see S1).

Comparison with other adsorption models at W|G. The main benefit of using the SD model is that it treats the lateral attraction in a more realistic way than the usual approach where a semi-empirical perturbation $-\beta\psi^2$ is made to the base EoS of particles without attraction (converting the Langmuir model to Frumkin, and HFL to Parsons [9]). To demonstrate this for $C_8\Phi E_m$ at W|G, we will compare the same

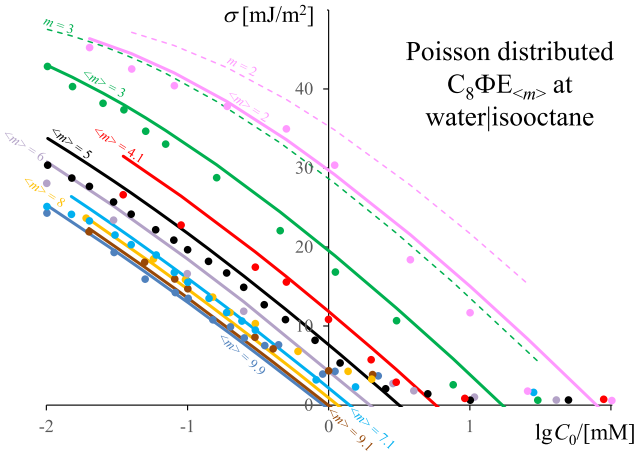

Fig. 4. Comparison of the LHP model (10)-(11) (solid lines) with data for interfacial tension vs total concentration before partitioning (points) for Poisson-distributed $C_8\Phi E_{<m>}$ on water|isooctane by Crook et al. [2]. The values of $< m >$ are indicated in the plot. The single-component HFL model (1)–(2) is shown for comparison for $m = 2$ and 3 (dashed lines).

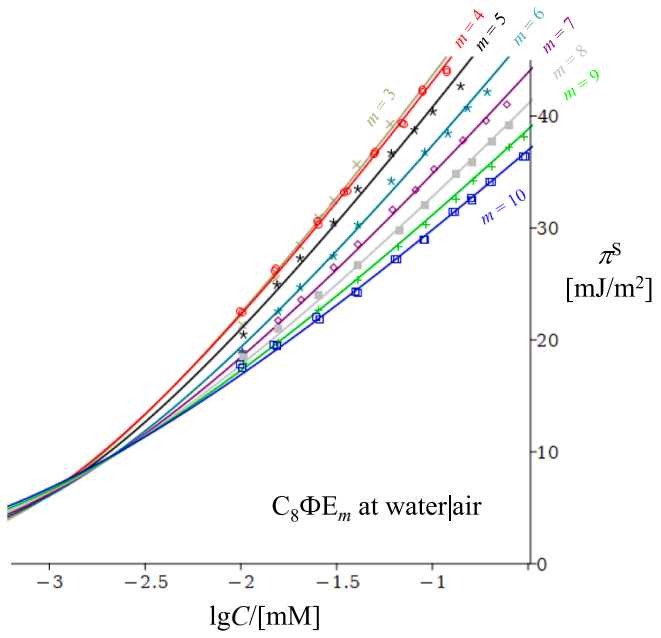

Fig. 5. Comparison of the SD model (3)–(5) with surface tension data for $C_8\Phi E_{3\text{-}10}$ on W|G from ref. [2].

data to the Parsons model (which is presented in S8).

We tried to keep the conditions of the regression close to that used for the SD model; however, an additional free parameter appears. The MTD model (17)–(19) for β is incompatible [9] with the Parsons model, so β must be treated as an empirical parameter to be determined from the data. For $\beta(m)$, we tried ten simple test functions and chose $\beta = \beta_1/m^{1/2}$ for the homologues of m = 6–10 (it produced the smallest deviation). The merit function is thus like (35) but with two parameters, K_{a0} and β_1, instead of just one. The optimization produced the values $\beta_1 = 10.5$ and $\ln(K_{a0}/[m]) = -7.47$ (different from the theoretical −6.3 from eq. (24)). Despite the additional fitting parameter, the Parsons model produces higher optimal deviation than SD (*dev* = 0.44 vs 0.36 mJ/m^2 for m = 6–10). The lateral attraction parameters of the Parsons model disagree significantly with the theoretically expected from Eqs. (17)–(19), see Fig. 6.

As with the SD model, the shorter homologues $C_8\Phi E_{3\text{-}5}$ were dealt with separately, due to the additional quadrupole attraction changing the trend in the isotherms. The comparison with the Parsons model with fixed $\ln(K_{a0}/[m]) = -7.47$ gives $\beta_5 = 4.81$, $\beta_4 = 5.40$, $\beta_3 = 5.64$.

The Parsons model has, however, one important advantage over SD: it has been generalized to mixtures [5].

Mixtures of $C_n\Phi E_m$ at W|G. Crook et al. reported the behaviour of the same mixtures we discussed above at W|O: binary $C_8\Phi E_4$ + $C_8\Phi E_{10}$ and nine Poisson distributed $C_8\Phi E_{<m>}$ at W|G. We compared them with the NPB model in S8, using the parameters of the single surfactants only (as obtained from the Parsons model). The results are reasonably good. The effect from the polydispersity of $C_8\Phi E_{<m>}$ is somewhat smaller compared to W|O.

Discussion of the adsorption parameters. The values of the adsorption parameters for both W|O and W|G are listed in Table 2 (the direct fitting MT parameters – K_{a0}, $x_\perp$, α_Φ) and Table 3 (actual values of K_a, α and β for each homologue, calculated via Eqs. (23), (14) and (17)–(19), except for $\beta_{3\text{-}5}$).

The results for the area are plotted in Fig. 6-left, where the disc area $\alpha(m)$ is compared with $\alpha_E(m)$ of the $-E_m$ segment and α_Φ of the $-C_2H_4-C_6H_4-O-C_2H_4-$ segment. The area $\alpha_\perp$ of neat interface lost upon adsorption from eq. (22) (which determines the dependence of K_a on m) is also shown for comparison. The important conclusion is that the geometry of the molecule in Fig. 1 translates directly into adsorption parameters of the homologous series at both W|O and W|G.

The dependence of β on m for W|G is illustrated in Fig. 6-right (at W|O, it is assumed that $\beta = 0$ and the HFL model holds instead of SD). For m = 6–10, the adsorption data at W|G are in excellent agreement with β from Eqs. (17)–(19) (blue circles). For m = 3–5, the data suggest much higher β (purple asterisks), probably due to benzene-benzene quadrupole interaction (see S2). For m = 1–2, the data suggest the monolayer is not fluid so we do not consider them.

The dependence of K_a on m from eq. (23) for W|O and W|G interfaces is shown in Fig. 7, with $x_\perp$ and $\ln K_{a0}$ from Table 2. The ratio of the slopes $d\ln K_a/dm$ at the two interfaces is equal to the ratio of σ_0 (i.e. $\sigma_0^{W|G}/\sigma_0^{W|O}$ = 72.0/50.1), resulting in a faster increase with m of K_a at W|G. The intercept difference is also captured well by the model (see Table 2).

***CMC* and solubilities.** One interesting application of the developed adsorption models is for analysis of the break in the σ vs C dependences

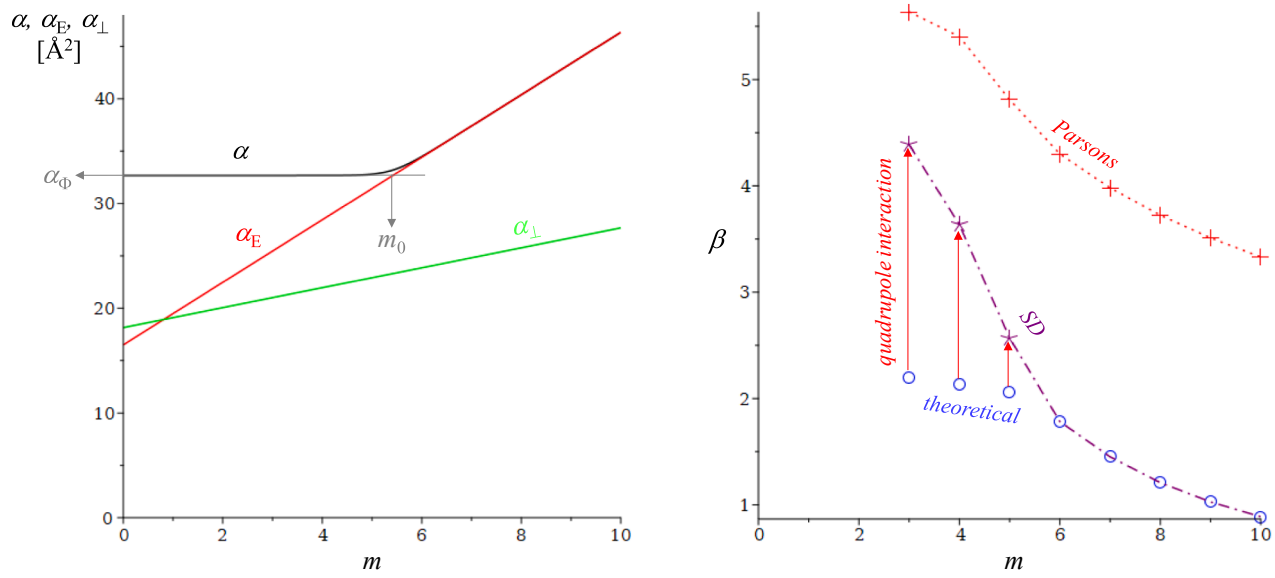

Fig. 6. Left: areas of $C_8\Phi E_m$ involved in the MTD models as functions of m: disc area α, eq. (14); area α_E of the $-E_m$ segment, see S1; penetration area $\alpha_\perp$, see Fig. 1 and eq. (22). **Right:** lateral attraction parameter of $C_8\Phi E_m$ at W|G. The higher homologues follow the model (17)-(19), but for m = 3–5 for which contact between the $-C_2H_4-C_6H_4-O-C_2H_4-$ segments is possible, β increases. The Parsons model's β values are shown for comparison.

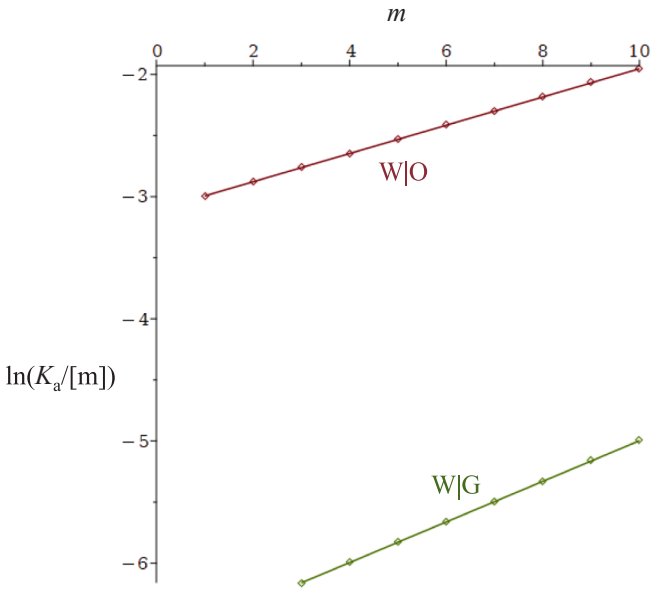

Fig. 7. Adsorption constants of the studied $C_8\Phi E_m$ homologues vs length m of the $-E_m$ chain, for W|O and W|G.

for $C_n\Phi E_m$ at W|G and W|O reported by Crook et al. [2] – it is presented in S4. In short, we show that we can use the plateau value of the surface/interfacial pressure to calculate the break point C_{break} very accurately. The increased accuracy allows us to identify which homologues reach a micellization point and which – a solubility limit – it appears that $C_8\Phi E_{1\text{-}4}$ do not form micelles. Moreover, this analysis gives additional evidence for 2D crystalline monolayer at W|G for $C_8\Phi E_{1\text{-}2}$.

4. Conclusions

Our theory of the adsorption of alkylphenyl polyethylene glycols, $C_n\Phi E_m$, at W|G and W|O interfaces, consists of **(i)** a family of adsorption hard-disc fluid equations of state (HFL [26], LHP [30], SD [27,6], NPB [5]) combined with **(ii)** MTD models (theoretical or from independent experiments) for the three adsorption parameters of these EoS: adsorption constants K_a, disc area α, and, at W|G, lateral attraction parameter β (based on ref. [6,10]). Nearly all parameters in the proposed theory are directly calculated or determined independently and have a clear physical meaning; only four molecular characteristics had to be determined from the experimental data: $\alpha_\Phi = 33$ Å^2, $x_\perp = 0.3$, $K_{a0} = \exp(-3.1)$ for W|O, $K_{a0} = \exp(-6.7)$ for W|G – see Table 2. These four values allow the prediction of the adsorption behaviour of any $C_n\Phi E_m$ homologue at W|G and W|O, and also the behaviour of surfactant mixtures. Even these four parameters can be estimated theoretically, and the estimates agree well with the values extracted from the data.

To our knowledge, this is the first adsorption theory that:

(i) predicts the behaviour of single and mixed polyethoxylates at W|O (Fig. 2, Fig. 3, Fig. 4), and that
(ii) captures quantitatively the phenomenon of intersection of the isotherms of short and long homologues at W|O (Fig. 2) and W|G (Fig. 5), based on MTD models for the adsorption parameters.

The proposed theory is exceptionally simple, in the sense that it is able to translate the geometry of the adsorbed molecule (Fig. 1, S1) directly to values of the adsorption parameters (Fig. 6) and thereafter into single and mixed adsorption isotherms. Excluding the geometry in Fig. 1, there are no new assumptions in the adsorption models compared to what was previously used for fluid monolayers of nonionic surfactants simpler than $C_n\Phi E_m$ [6,10]. The only exception is the need to accommodate the benzene ring attraction for three of the homologues, $C_8\Phi E_{3\text{-}5}$, at W|G. For comparison, previous adsorption modelling studies for alkylphenol surfactants at W|G (for example, ref. [13]) would use 3–4 parameters per homologue (when we need three for the whole series), with little discussion of the dependence of the adsorption parameters on m, and ignoring the polydispersity. To our knowledge, this work is also the first to propose theory for the excellent set of data reported by Crook et al. [1,2,17].

Perhaps the most important application of the proposed theory is to predict the behaviour of technical mixtures of ethoxylates. Obviously, commercial surfactants are mixtures [43]. We demonstrated this use on the example of nine Poisson distributed mixtures of $C_8\Phi E_m$ at W|O (see Fig. 4 and S9) and W|G (S8). To our knowledge, this is the first time this is done for liquid interfaces (it has been done before with solid surfaces [15,16]).

The proposed theoretical description provides a detailed picture of the properties of the adsorbed layers of $C_n\Phi E_m$, and the molecular thermodynamic reason behind the features of their behaviour. According to our findings,

(i) the lateral repulsion (the disc area α) is controlled by the $-E_m$ segment for $m \geq 6$ and by the $-C_2H_4-C_6H_4-O-C_2H_4-$ segment at $m \leq 5$. This results in W|O isotherms of similar shape at $m \leq 5$ but increasingly flatter π^S vs ln$C$ dependences at $m > 6$ (see Fig. 2 and S5).
(ii) The lateral attraction parameter β at W|G for $m \geq 6$ is dominated by the dispersion attraction, with some contribution from the osmotic effect due to water present in the monolayer. For $m \leq 5$, where the $-C_2H_4-C_6H_4-O-C_2H_4-$ segments can approach each other without the steric hindrance between $-E_m$ groups, β increases significantly (see Table 3 and Fig. 6-right), which we tentatively ascribe to short range quadrupole–quadrupole interaction between the benzene rings (see S2). For the shortest two homologues, the lateral cohesion becomes so strong that they 2D crystallize (see also S4).
(iii) The dependence of the free energy of adsorption $-kT\ln K_a$ on the size m of the polar head is linear. The predicted slope is controlled by the penetration area $\alpha_\perp$ (proportional to α_E) and the tension σ_0 of the surfactant-free interface (resulting in a different slope of $\ln K_a$ vs m for W|G and W|O, see Fig. 7 and Eq. (23)). The intercepts $\ln K_{a0}$ of this dependence at the two interfaces are also predicted with reasonable accuracy (see Table 2).

The next work from this series is to apply the same models to data for C_nE_m, where the phenylene segment is absent. A wide range of values of n (not only m) will be considered, and we will specify better the surface phase behaviour of this homologous series. We will also summarize the dependence of the partition coefficient K_p and the *CMC*/solubility on the structure of the C_nE_m surfactants (as done for $C_n\Phi E_m$ here in S3-4). In the third paper of the series, we will use a combination of adsorption, partition, micellization and solubility models to calculate the distribution of various C_nE_m surfactants in a complex system. We will show that this allows one to predict the behaviour of emulsions stabilized by these surfactants. A more challenging standing problem is the extension of the SD model to mixtures. It will be also interesting to apply the same models to liquid CO_2 emulsions, ethoxylated surfactants with branched alkyl [21,22] and related systems.

Declaration of Competing Interest

The authors declare the following financial interests/personal relationships which may be considered as potential competing interests: Radomir Slavchov reports financial support was provided by Sofia University St Kliment Ohridski. Radomir Slavchov reports financial support was provided by BASF SE.

Data availability

Data will be made available on request.

Acknowledgement

Dedicated to the memory of Prof. Ivan B. Ivanov (1935-2018), who had the vision of this work long before it was finished. Funding by BASF is gratefully acknowledged.

Appendix A. Supplementary data

S1. Disc area of the E_m segment and its relation to the hard disc area. **S2.** Lateral attraction parameter – dispersion and quadrupoles. **S3.** Partition coefficients. **S4.** State of the monolayer at the *CMC* / solubility limit. **S5.** Comparison between theory and data for single surfactants at W|O. **S6.** Comparison between theory and data for single surfactants at W|G. **S7.** Comparison between the adsorption behaviour of a mixture and the behaviour of the mean homologue at W|O. **S8.** The Parsons model for single component $C_8\Phi E_m$ and NPB for Poisson distributed $C_8\Phi E_{<m>}$ at W|G. **S9.** Procedure to calculate interfacial tension and composition for Poisson distributed $C_8\Phi E_{<m>}$. Supplementary data to this article can be found online at https://doi.org/10.1016/j.jcis.2023.06.068.

References

[1] E.H. Crook, D.B. Fordyce, G.F. Trebbi, J. Colloid Sci. 20 (1965) 191.
[2] E.H. Crook, D.B. Fordyce, G.F. Trebbi, J. Phys. Chem. 67 (1963) 1987.
[3] N. Nandi, J. Mol. Struct. (Theochem) 332 (1995) 301.
[4] M.J. Schick, S.M. Atlas, F.R. Eirich, J. Phys. Chem. 66 (1962) 1326.
[5] Y.J. Nikas, S. Puvvada, D. Blankschtein, Langmuir 8 (1992) 2680.
[6] R.I. Slavchov, I.B. Ivanov, J. Colloid Interface Sci. 532 (2018) 746.
[7] H. Lange, P. Jeschke, I.M.J. Schick (Eds.), Nonionic Surfactants. Physical Chemistry, Marcel Dekker Inc., New York, 1987.
[8] M.L. Pollard, R. Pan, C. Steiner, C. Maldarelli, Langmuir 14 (1998) 7222.
[9] R.I. Slavchov, I.B. Ivanov, Soft Matter 13 (2017) 8829.
[10] B. Peychev, R.I. Slavchov, J. Colloid Interface Sci. 594 (2021) 372.
[11] D. Seddon, E.A. Müller, J.T. Cabral, J. Colloid Interface Sci. 625 (2022) 328.
[12] C.G. Bell, C.J.W. Breward, P.D. Howell, J. Penfold, R.K. Thomas, Langmuir 23 (2007) 6042.
[13] V.B. Fainerman, R. Miller, E.V. Aksenenko, A.V. Makievski, in: V.B. Fainerman, D. Möbius, R. Miller (Eds.), Surfactants - Chemistry, Interfacial Properties, Applications, Elsevier, 2001 (Chapter 3).
[14] J. Viades-Trejo, J. Garcia-Fadrique, Fluid Phase Equilibria 464 (2008) 12.
[15] T.C.G. Kibbey, K.F. Hayes, J. Colloid Interface Sci. 197 (1998) 198–209.
[16] T.C.G. Kibbey, K.F. Hayes, J. Colloid Interface Sci. 197 (1998) 210–220.
[17] R.M. Weinheimer, P.T. Varineau, in: N.M. van Os (Ed.). Nonionic Surfactants: Organic Chemistry. Surfactant Science Series v. 72, 1997.
[18] B. Lalonde, C. Garron, Arch. Environ. Contam. Toxicol. 80 (2021) 319.
[19] J. Kang, C.M. Kim, D.Y. Yu, Y.S. Ham, S.K. Cho, J.J. Kim, Internat, J. Surface Eng. Coat. 97 (2018) 22, https://doi.org/10.1080/00202967.2019.1551276.
[20] D. Xing, B. Wei, W. McLendon, R. Enick, S. McNulty, K. Trickett, A. Mohamed, S. Cummings, J. Eastoe, S. Rogers, D. Crandall, B. Tennant, T. McLendon, V. Romanov, Y. Soong, SPE J. 17 (2012) 1172, https://doi.org/10.2118/129907-PA.
[21] L.C. Burrows, F. Haeri, D. Tapriyal, S. Sanguinito, P.G. Shah, P. Lemaire, D. Crandall, R.M. Enick, A. Goodman, Energy Fuels 36 (2022) (1929) 11913–11929.
[22] S. Cummings, R. Enick, S. Rogers, R. Heenan, J. Eastoe, Biochimie 94 (2012) 94–100.
[23] S. Patryka, S. Zaini, M. Lindheimer, B. Brun, Coll. Surf. 12 (1984) 255.
[24] R.I. Slavchov, S.I. Karakashev, I.B. Ivanov, in: L. Römsted (Ed.). Surfactant Science and Technology: Retrospects and Prospects, Taylor and Francis, LLC, 2014 (Chapter 2).
[25] J.N. Israelachvili, Intermolecular and Surface Forces, 3rd ed., Academic Press, 2011.
[26] E. Helfand, H.L. Frisch, J.L. Lebowitz, J. Chem. Phys. 34 (1961) 1037.
[27] T.D. Gurkov, I.B. Ivanov, in: Proc. 4th World Congress on Emulsions, Lyon, 2006, p. 509.
[28] I.B. Ivanov, K.D. Danov, D. Dimitrova, M. Boyanov, K.P. Ananthapadmanabhan, A. Lips, Coll. Surf. A 354 (2010) 118.
[29] R. Parsons, J. Electroanal. Chem. 7 (1964) 136–152.
[30] J.L. Lebowitz, E. Helfand, E. Praestgaard, J. Chem. Phys. 43 (1965) 774.
[31] D.P. Fraser, M.J. Zuckermann, O.G. Mouritsen, Phys. Rev. A 43 (1991) 6642.
[32] N.A. Grozev, T.G. Tosheva, I.M. Dimitrova, R.I. Slavchov, Bulg. J. Chem. 2 (2013) 25.
[33] M.N. Islam, T. Kato, Langmuir 21 (2005) 2419–2424.
[34] F. van Voorst Vader, F. Trans. Faraday Soc. 56 (1960) 1078.
[35] R. Sedev, Langmuir 17 (2001) 562.
[36] N.K. Adam, The Physics and Chemistry of Surfaces, Clarendon Press, 1941.
[37] I.B. Ivanov, K.P. Ananthapadmanabhan, A. Lips, Adv. Colloid Interface Sci. 123–126 (2006) 189.
[38] R.C. Mansfield, J.E. Locke, J. Am. Oil Chem. Soc. 41 (1964) 267–272.
[39] P.J. Flory, JACS 62 (1940) 1561–1565.
[40] R.I. Slavchov, I.M. Dimitrova, A. Menon, J. Chem. Phys. 151 (2019), 064502.
[41] I.L. Minkov, D. Arabadzieva, I.E. Salama, E. Mileva, R.I. Slavchov, Soft Matter 15 (2019) 1730.
[42] L. Sahoo, P.K. Misra, P. Somasundaran, Indian J. Chem. 41A (2002) 1402.
[43] N. Márquez, R.E. Antón, A. Usubillaga, J.L. Salager, J. Liquid Chromat. 17 (1994) 1147–1169.